

# Electronic Structure and Physicochemical Properties Characterization of the Amino Acids 12–26 of TP53: A Theoretical Study

Carolina Barrientos-Salcedo,<sup>\*,†,‡</sup> Diego Arenas-Aranda,<sup>†</sup> Fabio Salamanca-Gómez,<sup>†</sup> Rocío Ortiz-Muñiz,<sup>§</sup> and Catalina Soriano-Correa<sup>||</sup>

<sup>1</sup>Centro Médico Nacional Siglo XXI (CMN–SXXI), Instituto Mexicano del Seguro Social (IMSS), Cuauhtémoc, 06725 México, D.F., México<sup>2</sup>Laboratorio de Citometría de Flujo, Departamento de Ciencias de la Salud, Universidad Autónoma Metropolitana (UAM), Iztapalapa, 09340 México, D.F., México<sup>3</sup>Laboratorio de Química Computacional-QFB, Facultad de Estudios Superiores Zaragoza, Universidad Nacional Autónoma de México (UNAM), Iztapalapa, 09230 México, D.F., México

Received: November 26, 2006; In Final Form: February 6, 2007

PNC-27, a synthetic peptide, is derived from the TP53–HDM2 binding domain that include TP53 amino acids 12–26 linked with 17 amino acids from the *antennapedia* protein transference domain. This peptide induces membrane rupture in tumor cells through toroidal pores formation and has motivated several experimental studies; nonetheless, its mechanism of biological action remains unknown to date. Herein, we present a theoretical study at the Hartree–Fock and density functional theory (B3LYP) levels of theory of TP53 protein residues 12–26 (PPLSQETFSQDWKLL) in order to characterize its electronic structure and physicochemical properties. Our results for atomic and group charges, fitted to the electrostatic potential (ESP) show important reactive sites (L14, S15, T18, S20, L25, and L26), suggesting that these amino acids are exposed to nucleophilic and electrophilic attacks. Analysis of bond orders, intramolecular interactions and of several global reactivity descriptors, such as ionization potentials, hardness, electrophilicity index, dipole moments, total energies, frontier molecular orbitals (HOMO–LUMO), and electrostatic potential, led us to characterize active sites and the electronic structure and physicochemical features that taken together may be important in understanding the specific selectivity for this peptides type's cancer-cell membrane lysis properties.

## 1. Introduction

The use of peptides in cancer therapy has recently become popular due to their potency, specificity, low toxicity, and to the limitation of viral vector gene-therapy approaches.<sup>1,2</sup> An important requirement in peptide-therapy utilization is the ability of these molecules to be efficiently transduced across the cancer-cell membrane. In general, cellular membranes are largely impermeable to proteins; however, it has been shown that certain short peptide sequences possessing negatively or positively charged amino acids possess the facility not only of transporting themselves across cell membranes, but also of carrying attached molecules into the cells.<sup>3</sup>

Because of its significant role in tumorogenesis, the TP53 protein has long been a target for cancer therapy. The importance of TP53 prevention in cancer development is emphasized by the fact that >50% of clinically detected in human tumors have demonstrated mutations in one or both TP53 alleles. The p53

gene can also be inactivated by other mechanisms such as gain-of-function or overexpression.<sup>4,5</sup> Nevertheless, there are a number of cancers, particularly of glia, bone, and soft tissues, that have wild-type TP53 but that overexpress HDM2, a protein that can inhibit TP53's ability to bind to DNA and activate transcription.<sup>6,7</sup>

Kussie et al.<sup>8</sup> elucidated the X-ray crystal structure of the p53-MDM2 complex, Chi et al.<sup>9</sup> described details on mdm2–p53 interaction using heteronuclear multidimensional nuclear magnetic resonance (NMR) methods. Furthermore, Rosal et al.<sup>10</sup> employing two-dimensional NMR studied residues 12–26 of the human P53 region (PPLSQETFSQDWKLL) linked to penetratin, denominated PNC-27, that comprise amino acids in contact with HDM2 protein. Results showed that N-terminal portions of TP53 forms an amphiphatic  $\alpha$ -helix that inserts its hydrophobic face (Phe19, Trp23, and Leu26) into a deep groove in HDM2. Moreover, Rosal et al.<sup>11</sup> successfully used the protein transduction domains (PTD) linked with TP53 end regions-derived short peptide sequences to selectively destroy cancer cells. In addition, Do et al.<sup>12</sup> found that a amino-terminal p53 synthetic peptides induced nonapoptotic cell death resembling necrosis in breast-cancer cells. The authors also found that a synthetic peptide (Np53Ant-32) derived from N-terminal residues (12–26) of TP53 C-terminally linked with the same 17 amino acid PTD sequence induced TP53-independent necrosis in pancreatic cancer cells.<sup>13</sup> They studied several peptides from p53 amino terminal end domain and found that the fragment 17–20 (Glu-Thr-Phe-Ser) would appear essential for selective cytotoxic effects of the whole peptide containing residues 12–

\* Corresponding author: Carolina Barrientos S., UIM Genética Humana, Hospital de Pediatría, 2o piso, Av. Cuauhtémoc 330, Deleg. Cuauhtémoc, 06725 México, D.F., México. Telephone: (+52) (55) 5627-6941; Fax: (+52) (55) 5588-5174; E-mail addresses: carbasa@salud.gob.mx; socc@puma2.zaragoza.unam.mx

† Centro Médico Nacional Siglo XXI (CMN–SXXI), Instituto Mexicano del Seguro Social (IMSS).

‡ Doctorado en Ciencias Biológicas, Universidad Autónoma Metropolitana.

§ Laboratorio de Citometría de Flujo, Departamento de Ciencias de la Salud, Universidad Autónoma Metropolitana (UAM).

|| Laboratorio de Química Computacional-QFB, Facultad de Estudios Superiores Zaragoza, Universidad Nacional Autónoma de México (UNAM).

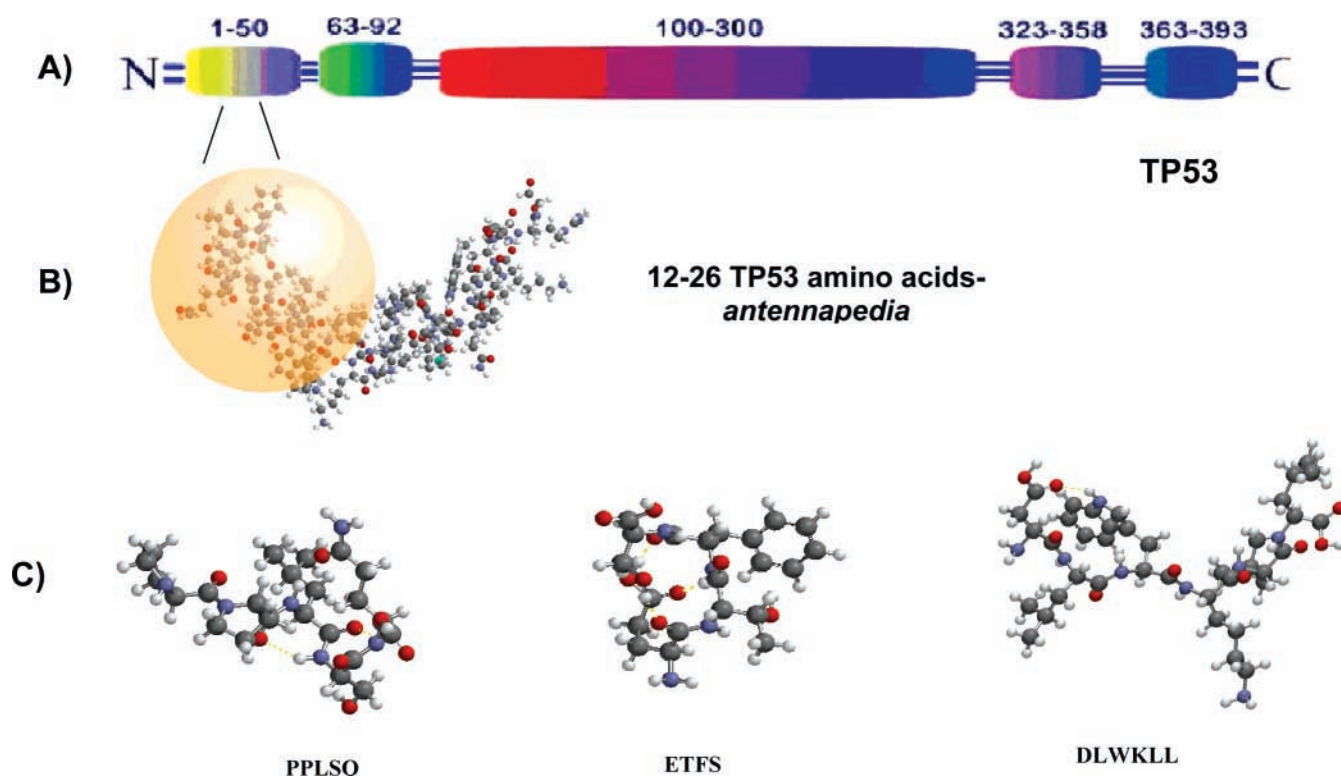


**Figure 1.** Images showing (A) TP53 protein, (B) amino acids 12–26 of TP53 protein (shaded circle) and penetratin, and (C) fragments analyzed in this study (ball and stick model).

26, so that of these four amino acids, two of these (Glu17 and Phe19) are binding residues between p53 and mdm2. In addition, these residues have also shown to be important in stabilizing the  $\alpha$ -helical conformation. Recently Mich et al.<sup>14</sup> described to PNC-28 peptide that contents ETFSDLWKLL amino acids of TP53 and that causes tumor-size decrease and slow tumor-growth increase. To the best of our knowledge, no ab initio studies have been performed to determine the electronic structure of TP53's 12–26 amino acids. Thus, the purpose of the present study was to undertake an ab initio study at the Hartree–Fock and density functional theory (B3LYP) levels of theory of the peptide sequence PPLSQETSDLWKLL carboxyl terminal ends for performing benchmark calculations to obtain structural and physicochemical parameters and several quantum-chemical descriptors. In addition, we characterize the electronic structure and physicochemical properties that might be associated with their selective cancer-cell membrane-lysis capacity by utilizing standard and complementary density descriptors to understand this type's behavior.

## 2. Theoretical Details

The chemical structure of the amino acids 12–26 (1Q2F, DOI: 10.2210/pdb1q2f/pdb)<sup>10</sup> studied in this work, was taken from the Protein Data Bank. Because PNC-27 has 15 amino acids deriving from TP53–HDM2 binding-domain 12–26 TP53 amino acids, according to the level calculation of this study, we consider the following three fragments: PPLSQ, ETFS, and DLWKLL (with carboxyl terminal ends in all cases). The chemical structures of the three fragments studied in this work are shown in Figure 1, while the atom-numbering for heavy atoms convention employed for these studies is shown in Figure 2. Geometric parameters optimization and electronic structure calculations were carried out in gas phase with the Gaussian 98 suite of programs.<sup>15</sup> The neutral structures were optimized at the Hartree–Fock (HF) level of theory, with a 6-31G(d) basis

set.<sup>16</sup> Subsequently, to gauge the electron correlation effect were performed single-point calculations on optimized structures at the density functional theory (DFT)<sup>17–19</sup> level of theory, using Becke's three parameters, and the correlation functional of Lee–Yang–Parr hybrid density functional (B3LYP),<sup>20–22</sup> implemented in the Gaussian 98 package of programs and with a 6-311G(d) basis set<sup>16</sup> to calculate atomic and amino acids group charges, fitted to the electrostatic potential (ESP),<sup>23</sup> for examining each amino acid's charges and reactive sites. Dipole moment analysis ( $\mu$ ) was performed at the same theory level to assess relative electronic charges of the amino acids segments. In addition, we performed a bond order analysis utilizing the natural bond orbital (NBO) scheme<sup>24–26</sup> at the same level of theory to provide an alternative insight into the relative acidity of amide and carboxyl-terminal end groups.<sup>27–29</sup> Furthermore, we determined frontier molecular orbitals (HOMO–LUMO) and electrostatic potential surfaces.<sup>23</sup> In addition, according to the Koopman theorem,<sup>30</sup> global reactivity descriptors such as ionization potential ( $I$ ), hardness ( $\eta$ ), and also the spatial extent measured though the  $\langle R^2 \rangle$  were calculated. Also, Parr et al.<sup>31</sup> have recently define a new descriptor to quantify the molecule's global electrophilic power as electrophilicity index ( $\omega$ ), which defines a quantitative classification of the global electrophilic nature of a molecule within a relative scale. Electrophilicity index of a system in terms of its chemical potential and hardness as

$$\omega = \frac{\mu^2}{2\eta} \quad (1)$$

In eq 1  $\mu \approx -(I + A)/2$  and  $\eta \approx (I - A)/2$  are the chemical potential and chemical hardness, respectively, approximated in terms of vertical ionization potential,  $I$ , and electron affinity,  $A$ . These descriptors have been defined within the density functional theory (DFT) context, and this index has been used

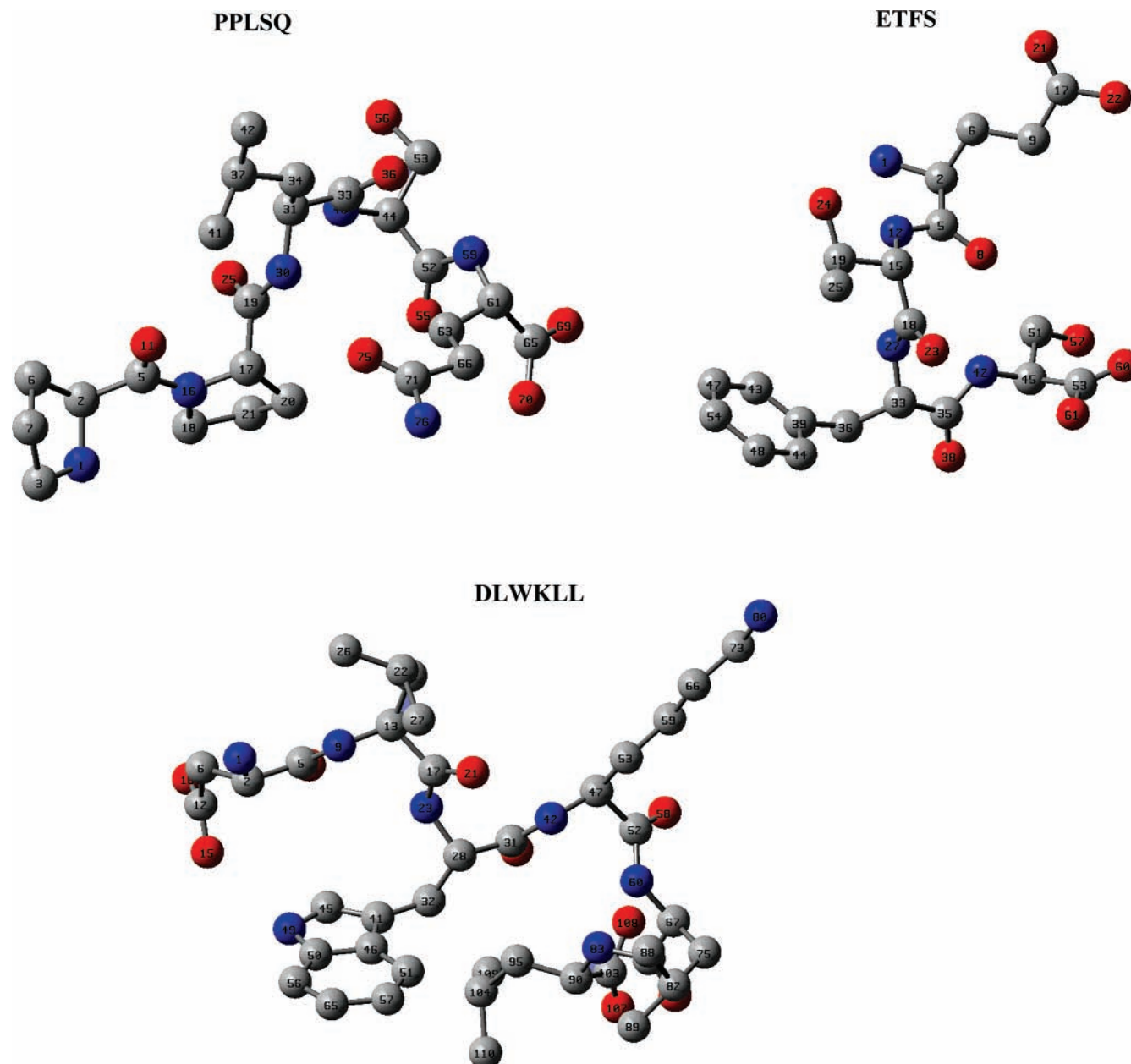


**Figure 2.** Convention used in numbering heavy atoms for analysis of atomic charges.

to explore variety of application including reactivity, toxicity and drug design.<sup>29,32–34</sup> Thus, we calculated the electrophilicity index ( $\omega$ ) at the same level of theory as the remainder of the previously mentioned global reactivity descriptors, to know the electrophilic nature of the fragments studied here.

### 3. Results and Discussion

The PNC-27 peptide derived amino acid sequence PPLSQETFSSDLWKLL (aa 12–26) was analyzed in three fragments (PPLSQ, ETFS, and DLWKLL)<sup>35</sup> as previously mentioned. In Table 1, we present atomic charges values (fitted to the ESP) for some selected atoms and amino acids of the fragments of PPLSQ, ETFS, and DLWKLL with carboxyl terminal ends, to explore whether atomic charges of atom and amino acid (aa 12–26) are related with the PNC-27 peptide's cancer cells selectivity membrane lysis. First, we investigated the effect of the charges on each full amino acid (amino acids including backbond and the side-chain atoms) in the fragments. Thus, we observe from Table 1 that the Q16 and S20 amino

acids possess the larger negative charges, these results suggesting that the more negative amino acids are exposed to a greater extent to electrophilic attacks on their respective fragments. In addition, it can be observed in Table 1 that the T18 amino acid has larger positive-charge values as compared with the remaining amino acids analyzed; therefore, nucleophilic-attacks might occur on this amino acid (i.e., this amino acid possess attractor properties). These results are consistent with the experimental result of Kanovsky et al.,<sup>13</sup> and reinforce the proposal that the segment (17–20, ETFS) is essential for the biological effect. Nonetheless, it may also be noted that charges values are significantly smaller than those of each amino acid reported in Table 1; thus, it is difficult to reach any definitive conclusion. Second place, we proceeded to analyze the effect of each atom's charges of all amino acids in the fragments, respectively, to analyze the nucleophilic or electrophilic nature of these sites (see Table 1). Hence, we observe in Table 1 that nitrogen atoms of amino acids Q16 ( $N_{76}$  and  $N_{59}$ ), K24 ( $N_{80}$ ), E17 ( $N_1$ ), D21 ( $N_1$ ), S20 ( $N_{42}$ ), and W23 ( $N_{23}$ ), respectively, possess larger

**TABLE 1: Atomic Charges for Some Selected Atoms and Amino Acids of the Fragments PPLSQ, ETFS, and DLWKLL of 12–26 Amino Acids of TP53 at the B3LYP/6-311G(d)//HF/6-31G(d) Level<sup>a</sup>**

P12	P13	L14	S15	Q16	E17	T18	F19	S20	D21	L22	W23	K24	L25	L26	
proline	proline	leucine	serine	glutamine	glutamic acid	threonine	phenylalanine	serine	aspartic acid	leucine	tryptophan	lysine	leucine	leucine	
0.009	0.057	-0.004	0.087	-0.148	-0.036	0.110	0.024	-0.098	0.023	0.058	0.003	-0.032	0.009	-0.061	
N <sub>1</sub>	C <sub>19</sub>	H <sub>32</sub>	N <sub>40</sub>	N <sub>59</sub>	N <sub>1</sub>	C <sub>18</sub>	N <sub>27</sub>	Precise Sites	N <sub>42</sub>	N <sub>1</sub>	O <sub>21</sub>	N <sub>23</sub>	H <sub>48</sub>	C <sub>82</sub>	N <sub>83</sub>
-0.684	0.739	0.326	-0.655	-0.919	-1.008	0.629	-0.661		-0.714	-0.937	-0.465	-0.703	0.230	0.593	-0.659
O <sub>25</sub>	C <sub>33</sub>	H <sub>45</sub>	H <sub>62</sub>	H <sub>4</sub>	O <sub>24</sub>	C <sub>35</sub>	H <sub>46</sub>	C <sub>12</sub>	C <sub>22</sub>	C <sub>31</sub>	C <sub>52</sub>	C <sub>52</sub>	H <sub>94</sub>		
-0.595	0.634	0.374	0.409	0.370	-0.659	0.572	0.350	0.836	0.548	0.555	0.526	0.327			
O <sub>36</sub>	C <sub>52</sub>	C <sub>65</sub>	O <sub>8</sub>	H <sub>29</sub>	C <sub>53</sub>	O <sub>15</sub>	O <sub>40</sub>	N <sub>80</sub>					C <sub>103</sub>		
-0.545	0.726	0.577	-0.547	0.419	0.682	-0.628	-0.562	-1.034					0.686		
C <sub>37</sub>	O <sub>56</sub>	C <sub>71</sub>	C <sub>17</sub>	H <sub>60</sub>	O <sub>75</sub>	H <sub>28</sub>	O <sub>57</sub>	O <sub>16</sub>	H <sub>61</sub>	H <sub>91</sub>					
0.534	-0.645	0.953	0.789	0.406	-0.637	0.448	-0.705	-0.640	0.380	0.378					
			N <sub>76</sub>				H <sub>63</sub>	H <sub>20</sub>							
			-1.064				0.429	0.456							

<sup>a</sup> Values of the atomic and amino acids charges are given in au.

**TABLE 2: Reactivity and Density Descriptors for Fragments of 12–26 Amino Acids of TP53 at the B3LYP/6-311G(d)//HF/6-31G(d) Level**

fragment	I <sup>a</sup> (eV)	$\eta^a$ (eV)	$\omega^a$ (eV)	$\langle R^2 \rangle$ (au)	-energy (au)
PPLSQ	5.85	2.89	1.51	21 432	1869.48006
ETFS	6.59	3.06	2.03	18 105	1714.81365
DLWKLL	5.72	2.62	1.84	48 785	2639.28166

<sup>a</sup> I,  $\eta$ , and  $\omega$  were calculated by using Koopman's theorem<sup>30</sup>

negative charges on nitrogen atoms of the amide groups, suggesting that more negative nitrogen atoms are more exposed to electrophilic attacks on these atoms than on the remainder of nitrogen atoms. Regarding carbonyl groups, we observed (Table 1) (Figure 2) that oxygen atoms such as S20 (O<sub>57</sub>), T18 (O<sub>24</sub>), S15 (O<sub>56</sub>), D21 (O<sub>15</sub> and O<sub>16</sub>), and Q16 (O<sub>75</sub>) have larger negative charges on carbonyl end groups oxygen atoms as compared with the remainder of the atoms; therefore, electrophilic attacks might occur on these sites as well. Furthermore, in Table 1 we observe that carbon atoms Q16 (C<sub>71</sub>), D21 (C<sub>12</sub>), E17 (C<sub>17</sub>), P13 (C<sub>19</sub>), L26 (C<sub>103</sub>), S15 (C<sub>52</sub>), S20 (C<sub>53</sub>), L14 (C<sub>33</sub>), T18 (C<sub>18</sub>), and L25 (C<sub>82</sub>) possess larger positive charges as compared with the remainder of the atoms; thus, nucleophilic-attacks could also occur on these sites. Addition, this result is in agreement with the more plentiful negative charges observed in the previously mentioned oxygen atoms.

In Table 2, we tabulated certain calculated global reactivity descriptors values for the fragments, such as ionization potential (I), hardness ( $\eta$ ), electrophilicity index ( $\omega$ ), and a density descriptor such as  $\langle R^2 \rangle$ . It can be observed that the ETFS fragment exhibits a larger value for ionization potential, which might be related with the greater global chemical stability of these fragments, i.e., larger relative values may indicate smaller oxidative effects, and we observe that PPLSQ and DLWKLL show a decreasing potential order. This is in fair agreement with our results for the global hardness descriptor, in that a less reactive fragment should possess larger hardness values, i.e., PPLSQ and DLWKLL fragments demonstrate a decreasing hardness order when these fragments are compared with the ETFS fragment. Furthermore, electrophilicity index values indicate that the ETFS fragment possesses a larger global electrophilic capacity than DLWKLL and PPLSQ, this in agreement with the observation previously discussed concerning ETFS-fragment charges, which would increase electrophilic-attack susceptibility. From  $\langle R^2 \rangle$  density-descriptor values, we are able to obtain a spatial extent measurement of these fragments and note that, for instance, the ETFS fragment is

**TABLE 3: Total Dipole Moment Values and Components for the Selected Fragments of 12–26 Amino Acids of TP53 at the B3LYP/6-311G(d)//HF/6-31G(d) Level<sup>a</sup>**

fragment	$\mu(x)$	$\mu(y)$	$\mu(z)$	$\mu(\text{total})$
PPLSQ	-2.07	-4.50	5.02	7.05
ETFS	0.21	-5.51	0.51	5.54
DLWKLL	-13.86	3.46	-1.28	14.34

<sup>a</sup> The total dipole moment values and its components are given in Debye

much more compact as compared with DLWKLL, this in agreement with its larger hardness value.

Dipole-moment ( $\mu$ ) analysis was carried out to assess the electronic charge on the x, y, and z axes of each amino acid. In Table 3, we tabulated the values of total dipole moments along with their components for studied fragments, and observed that PPLSQ and ETFS fragments possess smaller values. We may note from the results for dipole-moment components that the DLWKLL fragment has the larger negative value on the x axis, indicating that the negative charge is oriented toward the fragment's L22 and W23 amino acids, this in agreement with the previously discussed observation regarding atomic charges. Another interesting observation comprises the fact that the ETFS fragment possesses the larger positive value on the x axis, indicating that the positive charge is oriented toward the E17 amino acid. This observation may be associated with the interesting sites of interaction (i.e., reactive sites within the chemical reactivity framework) with the cell membrane, this in agreement with observations discussed previously concerning atomic charges and the electrophilicity index (Tables 1 and 2) and the experimental observation.<sup>10,13</sup>

Otherwise, we analyzed bond order to explore the relative acidity of certain selected amide-group hydrogen atoms. We may further comment on amide-groups acidity by analyzing N–H bond orders, because a smaller bond order should be indicative of a more acidic group.<sup>21–24</sup> On considering PPLSQ fragments, we found two interesting bond orders: N<sub>30</sub>–H<sub>32</sub> (0.676), and N<sub>59</sub>–H<sub>62</sub> (0.678). Whereas the ETFS fragment showed only one N<sub>42</sub>–H<sub>46</sub> (0.699) and the DLWKLL fragment finally had three bond orders [N<sub>42</sub>–H<sub>48</sub> (0.693), N<sub>83</sub>–H<sub>94</sub> (0.702), and N<sub>49</sub>–H<sub>61</sub> (0.711)], these results show that the PPLSQ fragment possesses smaller values of N–H bond orders, evidence that the PNC-27 amino acid possesses acidic groups that could be important interaction sites. It is noteworthy that deprotonation-energy calculations may provide alternative meth-

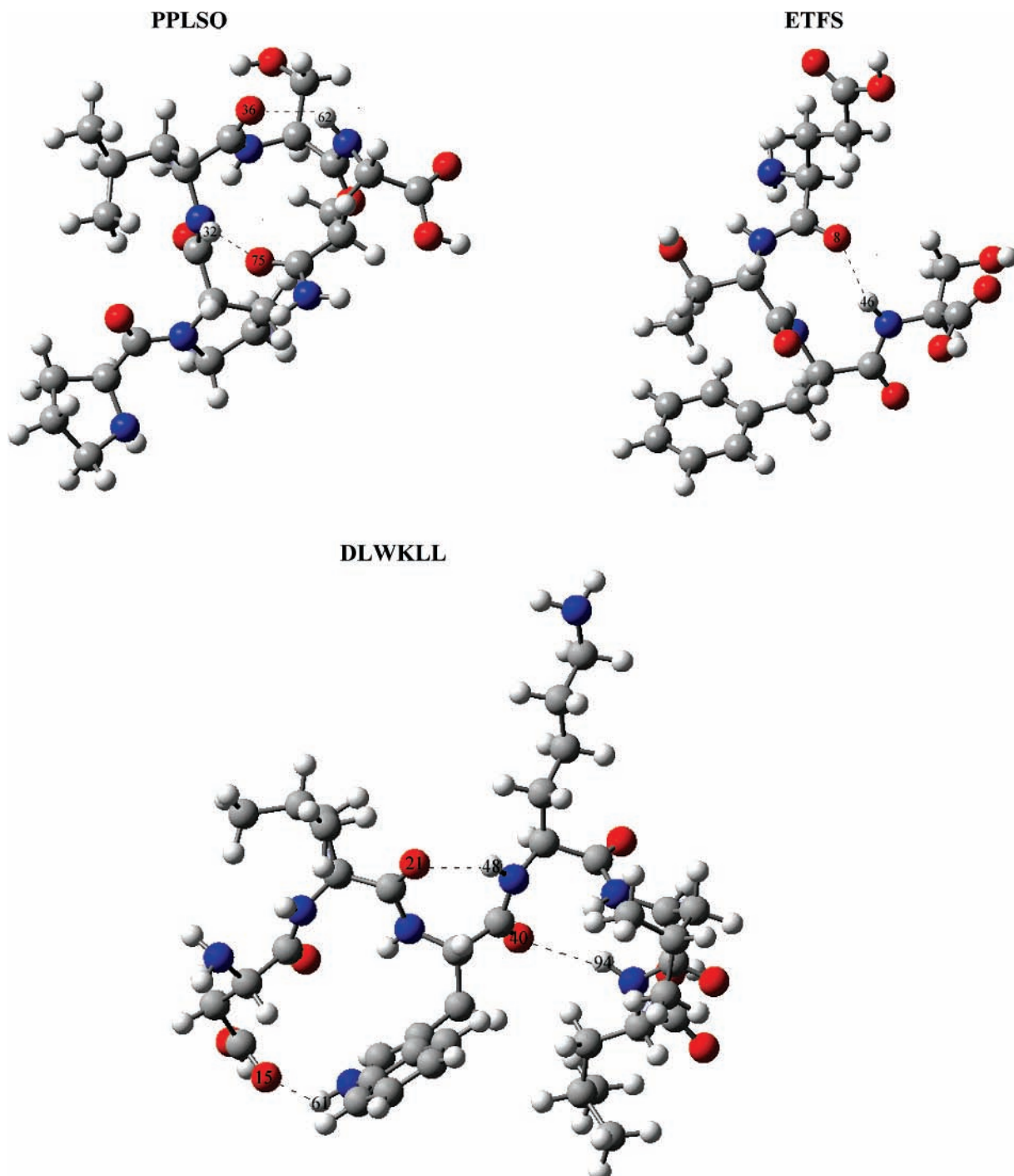


**Figure 3.** Optimized structures illustrate the possibility of forming an intramolecular hydrogen bond.

ods of analyzing amide-groups acidity through hydrogen atom (H) strength, as has been studied in previous works.<sup>27–29</sup> Efforts have been undertaken in our laboratory to support our conjecture regarding the relationship between the hydrogen atom's acidic nature and biological activity. Nevertheless, due to size of these structures we calculated bond order as one indirect method for analyzing relative amide-groups acidity. Another interesting feature that may be observed from the previously mentioned hydrogen atom charges is that these have a larger positive charge (see Table 1); thus, these atoms could be forming hydrogen bonds for the PPLSQ fragment  $\text{NH}_{32}\cdots\text{O}_{75}\text{C}$ , as can be observed in  $R_{(\text{H}_{32}\cdots\text{O}_{75})}$  a distance whose value is 2.31 Å. In addition, similar behavior is found for the remainder of hydrogen bonds  $\text{NH}_{62}\cdots\text{O}_{36}\text{C}$ ,  $R_{(\text{H}_{62}\cdots\text{O}_{36})}$  distance value is 2.09 Å. ETFS fragment

$\text{NH}_{46}\cdots\text{O}_8\text{C}$ ,  $R_{(\text{H}_{46}\cdots\text{O}_8)}$  distance value is 2.16 Å, while DLWKLL fragment  $\text{NH}_{48}\cdots\text{O}_{21}\text{C}$ ,  $R_{(\text{H}_{48}\cdots\text{O}_{21})}$  distance value is 2.10 Å;  $\text{NH}_{94}\cdots\text{O}_{40}\text{C}$ ,  $R_{(\text{H}_{94}\cdots\text{O}_{40})}$  distance value is 2.35 Å, and  $\text{NH}_{61}\cdots\text{O}_{15}\text{C}$ ,  $R_{(\text{H}_{61}\cdots\text{O}_{15})}$  distance value is 2.36 Å (see Table 1 and Figure 3). Analyzing these intramolecular interactions, it can be observed that all these distances values are shorter than the van der Waals radii.<sup>36–39</sup> It is noteworthy that these results are reinforced with the larger positive charges and the hydrogen atoms' relative acidity<sup>27–29</sup> (see Table 1 and Figure 3). These results additionally suggest that the presence of hydrogen bonds may contribute to increasing in the DLWKLL-fragment structure stability and  $\alpha$ -helix.<sup>11</sup> In Figure 4, the frontier molecular orbitals (HOMO and LUMO) in each analyzed fragment are shown. The results illustrate that for the PPLSQ amino acids segment,

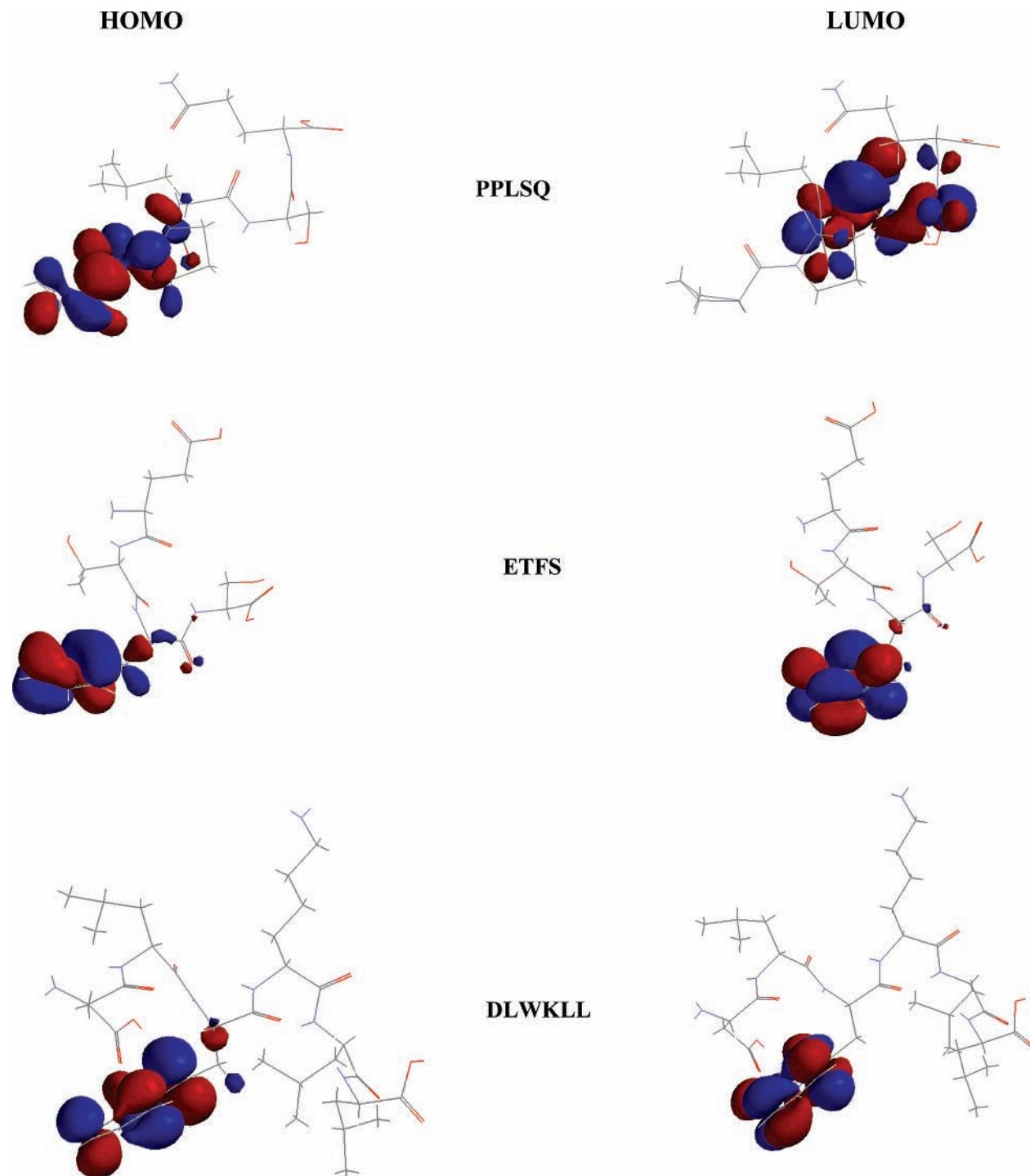


**Figure 4.** Frontier molecular orbitals (HOMO and LUMO) determined for PPLSQ, ETFS, and DLWKLL fragments of the aa 12–26 peptide.

the frontier molecular orbitals (HOMO) are located in the proline 12 and proline 13 amino acids. On the other hand, the molecular orbitals (LUMO) are located in leucine 14 and serine 15 amino acids. Furthermore, in Figure 4 we may observe that the molecular orbitals (HOMO and LUMO) are situated in phenylalanine 19 in the ETFS segment. Further, the results illustrate that frontier molecular orbitals (HOMO and LUMO) are located in tryptophan 23 in the DLWKLL segment. These results suggest the existence of a possible reactive site on the previously mentioned amino acids; therefore, nucleophilic or electrophilic attacks might take place on these sites as well. Finally, we analyzed electrostatic potential surfaces for PPLSQ, ETFS, and DLWKLL fragments, the results illustrating a larger distribution

of electronic density on carboxyl terminal ends in all fragments, as shown in Figure 5.

#### 4. Conclusions

We performed an ab initio study at the Hartree–Fock and density functional theory (B3LYP) levels of theory for some selected fragments (PPLSQ, ETFS, and DLWKLL) of the amino acids 12–26 deriving from PNC-27 to characterize the most relevant electronic and structural parameters and their physicochemical features that might be linked to their selective cancer cells membrane lysis. Our results revealed that PPLSQ, ETFS, and DLWKLL fragments studied herein have important electrophilic sites such as Q16 ( $C_{71}$ ), D21 ( $C_{12}$ ), E17 ( $C_{17}$ ), P13

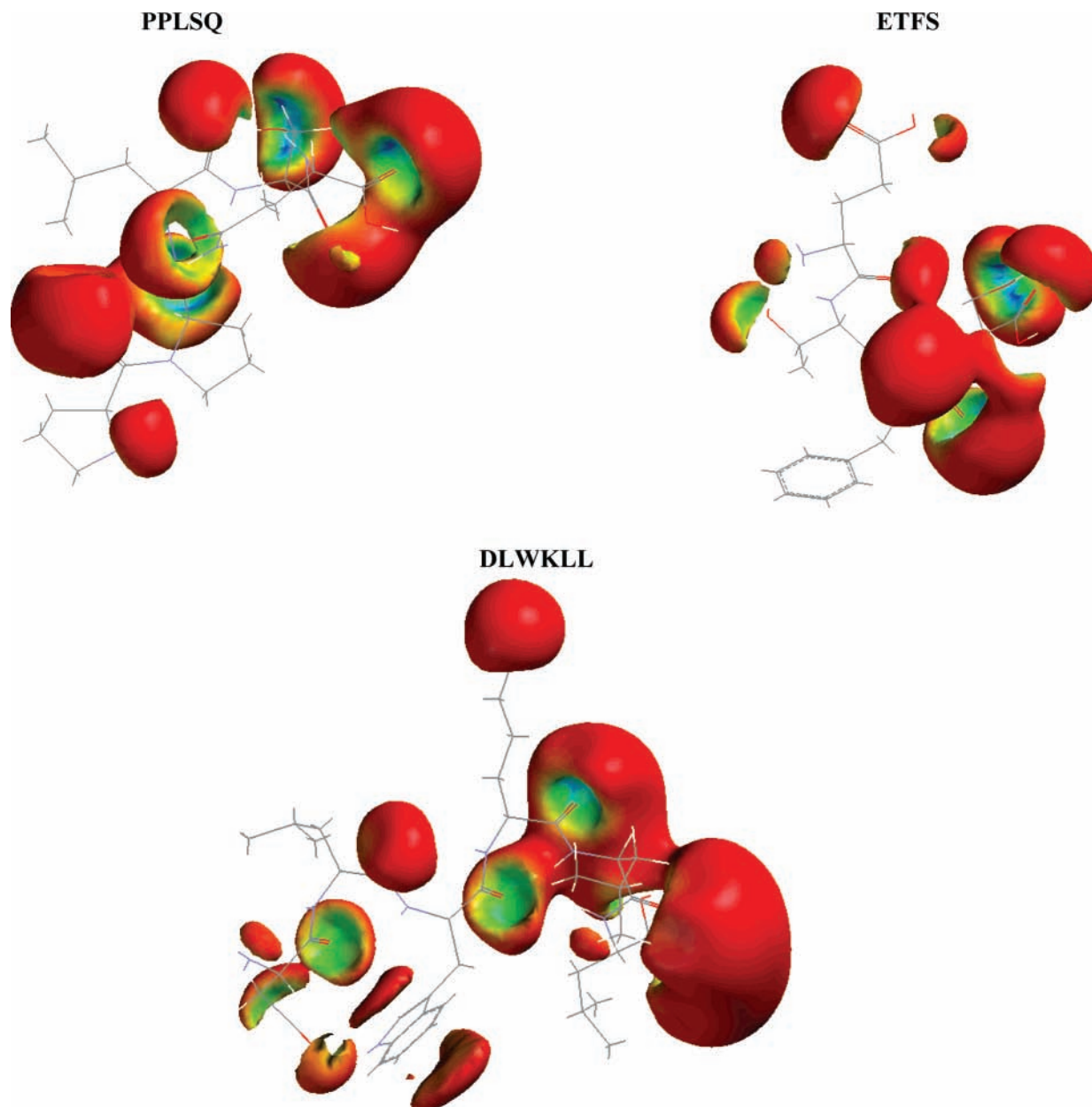


**Figure 5.** Electrostatic potential surfaces showing electronic density for PPLSQ, ETFS, and DLWKLL fragments of the aa 12–26 peptide.

(C<sub>19</sub>), L26 (C<sub>103</sub>), S15 (C<sub>52</sub>), S20 (C<sub>53</sub>), L14 (C<sub>33</sub>), T18 (C<sub>18</sub>), and L25 (C<sub>82</sub>), suggesting that these amino acids are exposed to nucleophilic attacks on these atoms. Also, from the negative charge on nitrogen atoms such as Q16 (N<sub>76</sub> and N<sub>59</sub>), K24 (N<sub>80</sub>), E17 (N<sub>1</sub>), D21 (N<sub>1</sub>), S20 (N<sub>42</sub>), and W23 (N<sub>23</sub>) and oxygen atoms S20 (O<sub>57</sub>), T18 (O<sub>24</sub>), S15 (O<sub>56</sub>), D21 (O<sub>15</sub> and O<sub>16</sub>), and Q16 (O<sub>75</sub>), respectively, we observed that these have larger negative charges as compared with the remainder of the atoms; therefore, electrophilic attacks might occur on these sites as well.

As an alternate means for evaluating the properties of these peptides, we employed global reactivity descriptors, from which we could assess the global chemical reactivity and the structural stability of these peptides from ionization potentials and hardness values, respectively. In addition, from electrophilicity indexes values we were able to study the global electrophilic capacity. Results of the relative acidity of amide groups by analysis of N–H bond orders showed that the PPLSQ fragment possesses the smallest values of all fragments, providing evidence that the (PPLSQETFSQLWKLL) amino acid possesses acidic groups that may be important reactive sites. Another interesting feature

related with hydrogen atom charges is that these atoms might be forming hydrogen bonds (i.e., intramolecular interactions), which might contribute to increasing the structure stability of these peptides. Furthermore, results of the frontier molecular orbitals (HOMO–LUMO) and electrostatic potential surfaces revealed possible reactive sites of amino acid fragment. Finally, our results illustrate that structural and electronic characterization as well as physicochemical properties obtained through theoretical study may contribute to understanding the behavior of these molecules.

**Acknowledgment.** We are grateful to the Dirección General de Servicios de Cómputo Académico at the Universidad Nacional Autónoma de México and the Laboratorio de Supercomputo y Visualización en Paralelo at the Universidad Autónoma Metropolitana-Iztapalapa for allocation of computer time. This research was partially supported by PAPIIT-UNAM Grant No. IN109206. Carolina Barrientos Salcedo thanks to Doctorado en Ciencias Biológicas at the Universidad Autónoma Metropolitana.

## References and Notes

- (1) Villanueva, J.; Martorella, A. J.; Lawlor, K.; Philip, J.; Fleisher, M.; Robbins, R. J.; Tempst, P. *Mol. Cell Proteomics* **2006**, *5*, 1840.
- (2) Sherr, C. J. *Cell* **2004**, *116*, 235.
- (3) Wadia, J. S.; Dowdy, S. F. *Curr. Opin. Biotechnol.* **2002**, *13*, 52.
- (4) Fleischer, A.; Ghadiri, A.; Dessauge, F.; Duhamel, M.; Rebollo, M. P.; Alvarez-Franco, F.; Rebollo, A. *Mol. Immunol.* **2006**, *43*, 1065.
- (5) Van, D. T. *Nature (London)* **2005**, *434*, 287.
- (6) Haupt, Y.; Maya, R.; Kazaz, A.; Oren, M. *Nature* **1997**, *387*, 296.
- (7) Kubbutat, M. H. G.; Jones, S. N.; Vousden, K. H. *Nature* **1997**, *387*, 299.
- (8) Kussie, P. H.; Gorina, S.; Marechal, V.; Elenbaas, B.; Moreau, J.; Levine, A. J.; Pavletich, N. P. *Science* **1996**, *274*, 948.
- (9) Chi, S. W.; Lee, S. H.; Kim, D. H.; Ahn, M. J.; Kim, J. S.; Woo, J. Y.; Torizawa, T.; Kainoshio, M. K.; Han, K. H. *J. Biol. Chem.* **2005**, *46*, 38795.
- (10) Rosal, R.; Pincus, M. R.; Brandt-Rauf, P. W.; Fine, R. L.; Michl, J.; Wang, H. *Biochemistry* **2004**, *43*, 1854.
- (11) Rosal, R.; Brandt-Rauf, P.; Pincus, M. R.; Wang, H.; Mao, Y.; Li, Y.; Fine, R. L. *Adv. Drug. Deliv. Rev.* **2005**, *57*, 653.
- (12) Do, T. N.; Rosal, R. V.; Drew, L.; Raffo, A. J.; Michl, J.; Pincus, M. R.; Friedman, F. K.; Petrylak, D. P.; Cassai, N.; Szmulowicz, J.; Sidhu, G.; Fine, R. L.; Brandt-Rauf, P. W. *Oncogene* **2003**, *22*, 1431.
- (13) Kanovsky, M.; Raffo, A.; Drew, L.; Rosal, R.; Drew, L.; Do, T.; Friedman, F. K.; Rubinstein, P.; Visser, J.; Robinson, R.; Brandt-Rauf, P. W.; Michl, J.; Fine, R. L.; Pincus, M. R. *Proc. Natl. Acad. Sci. U.S.A.* **2001**, *98*, 12438.
- (14) Michl, J.; Scharf, B.; Schmidt, A.; Huynh, C.; Hannan, R.; von Gizecki, H.; Driedman, F.; Brandt-Rauf, P.; Fine, R.; Pincus, M. *Int. J. Cancer* **2006**, *119*, 1577.
- (15) (a) Frisch, M. J.; Trucks, G. W.; Schlegel, H. B.; Scuseria, G. E.; Robb, M. A.; Cheeseman, J. R.; Zakrzewski, V. G.; Montgomery, J. A., Jr.; Stratmann, R. E.; Burant, J. C.; Dapprich, S.; Millam, J. M.; Daniels, A. D.; Kudin, K. N.; Strain, M. C.; Farkas, O.; Tomasi, J.; Barone, V.; Cossi, M.; Cammi, R.; Mennucci, B.; Pomelli, C.; Adamo, C.; Clifford, S.; Ochterski, J.; Petersson, G. A.; Ayala, P. Y.; Cui, Q.; Morokuma, K.; Malick, D. K.; Rabuck, A. D.; Raghavachari, K.; Foresman, J. B.; Cioslowski, J.; Ortiz, J. V.; Baboul, A. G.; Stefanov, B. B.; Liu, G.; Liashenko, A.; Piskorz, P.; Komaromi, I.; Gomperts, R.; Martin, R. L.; Fox, D. J.; Keith, T.; Al-Laham, M. A.; Peng, C. Y.; Nanayakkara, A.; Challacombe, M.; Gill, P. M. W.; Johnson, B.; Chen, W.; Wong, M. W.; Andrés, J. L.; González, C.; Head-Gordon, M.; Replogle, E. S.; Pople, J. A. Gaussian 98. Revision A.6, Gaussian: Pittsburgh, PA, 1998. (b) The theoretical calculations were carried out with the package of electronic structure Gaussian 98, Revision A.6. We used workstation and cluster (180 processors and 700 Gigaflops), the computer platform is Linus, and the Operating System is CentOS, version 4.4 with kernel 2.6.9-42.
- (16) Hehre, W. J.; Radom, L.; Schleyer, P. V. R.; Pople, J. A. *Ab initio Molecular Orbital Theory*; John Wiley & Sons: New York, 1986.
- (17) Hohenberg, P.; Kohn, W. *Phys. Rev.* **1964**, *136*, B864.
- (18) Kohn, W.; Sham, L. *J. Phys. Rev.* **1965**, *140*, A1133.
- (19) Parr, R. G.; Yang, W. *Density-Functional Theory of Atoms and Molecules*; Oxford University Press: New York, 1989.
- (20) Becke, A. D. *Phys. Rev. A* **1988**, *38*, 3098.
- (21) Becke, A. D. *J. Chem. Phys.* **1993**, *98*, 5648.
- (22) Lee, C.; Yang, W.; Parr, R. G. *Phys. Rev. B* **1988**, *37*, 785.
- (23) Politzer, P.; Truhlar, D. G. *Chemical Applications of Atomic and Molecular Electrostatic Potentials*; Academic Press: New York, 1981.
- (24) Reed, A. E.; Weinhold, F. *J. Chem. Phys.* **1983**, *78*, 4066.
- (25) Reed, A. E.; Weinstock, R. B.; Weinhold, F. *J. Chem. Phys.* **1985**, *83*, 735.
- (26) Carpenter, J. E.; Weinhold, F. *J. Mol. Struct. (THEOCHEM)* **1988**, *169*, 41.
- (27) Soriano-Correa, C.; Esquivel, O. R.; Sagar, R. P. *Int. J. Quantum Chem.* **2003**, *94*, 165.
- (28) Soriano-Correa, C.; Sánchez-Ruiz, J. F.; Rico-Rosillo, G.; Giménez-Scherer, J. A.; Velázquez, J. R.; Kretschmer, R. R. *J. Mol. Struct. (THEOCHEM)* **2006**, *769*, 91.
- (29) Soriano-Correa, C.; Sánchez-Ruiz, J. F.; Raya, A.; Esquivel, O. R. *Int. J. Quantum Chem.* **2007**, *107*, 628.
- (30) Koopmans, T. A. *Physica* **1933**, *1*, 104.
- (31) Parr, R. G.; Szentpály, L. V.; Liu, S. *J. Am. Chem. Soc.* **1999**, *121*, 1922.
- (32) Parthasarathi, R.; Subramanian, V.; Roy, D. R.; Chattaraj, P. K. *Bioorg. Med. Chem.* **2004**, *12*, 5533.
- (33) Sarkar, U.; Padmanabhan, J.; Parthasarathi, R.; Subramanian, V.; Chattaraj, P. K. *J. Mol. Struct. (THEOCHEM)* **2006**, *758*, 119.
- (34) Contreras, R.; Andrés, J.; Domingo, L. R.; Castillo, R.; Pérez, P. *Thetrahedron* **2005**, *61*, 417.
- (35) The detailed geometric structures are available from the authors upon request.
- (36) Pauling, L. *The Nature of the Chemical Bond*; Cornell University Press: Ithaca, NY, 1960.
- (37) Schuster, P.; Zundel, G.; Sandorf, C., Ed.; *The Hydrogen Bond/I Theory*; North-Holland Publishing Co.: Amsterdam, The Netherlands, 1976.
- (38) Oliveira, B. G.; Vasconcellos, M. L. A. A. *J. Mol. Struct. (THEOCHEM)* **2006**, *774*, 83.
- (39) Liu, G.; Wang, H.; Li, W. *J. Mol. Struct. (THEOCHEM)* **2006**, *772*, 103.